

## A laboratory model of thermally-driven marginal seas

Masaki TAKEMATSU\*

**Abstract:** Here we describe a new laboratory experiment which has been designed to study the possible effects of the differential cooling of the Japan Sea on the Tsushima Current system. The laboratory model consists of a cylindrical basin of uniform depth placed centrally in a larger tank; the inner basin ('the Japan Sea') is connected to the outer tank through two shallow passages on the western and eastern side of the basin. The fluid motion in the model is driven by cooling the northern portion of the basin's sidewall. By means of a dye technique it is observed that the localized sinking of cold water along the northern sidewall, combined with (constant) Coriolis forces and damping effects, gives rise to not only an intense western boundary current in the inner basin but also an inflow through the western passage (the 'Korea/Tsushima Strait') and a compensating outflow through the eastern passage (the 'Tsugaru Strait'). A feature of the buoyancy-driven inflow through the 'Korea/Tsushima Strait' is that its volume transport tends to concentrate in the northern part of the Strait.

In some experimental runs the eastern passage is closed to model the Mediterranean Sea with the Strait of Gibraltar. In this case the differential cooling of the inner basin induces a surface inflow through the single western passage; the surface inflow is replaced by a compensating lower-layer outflow from the inner basin.

### 1. Introduction

A major feature of the current system in the Japan Sea is the inflow of the Tsushima Current through the Korea/Tsushima Strait and the outflow through the Tsugaru Strait. This in- and outflow phenomenon in the Japan Sea is generally thought to be caused by the pressure (sea-level) difference associated with the Kuroshio current system in the North Pacific Ocean (cf. MINATO and KIMURA, 1980; TOBA *et al.*, 1982; SEKINE, 1988; FANG *et al.*, 1991). As noted by MINATO and KIMURA (1980), however, the pressure difference in the open ocean is merely one of possible factors causing the in- and outflow of the marginal sea: Other relevant factors include the differential cooling and the wind forcing over the Japan Sea. Indeed, a previous laboratory study of TAKEMATSU (1991) suggested that a localized sinking of cold water due to differential cooling of an ocean basin might strongly affect the in- and outflow process through openings (or an opening) of the basin. The

objective of the present study is to confirm this suggestion in a suitable laboratory model.

The laboratory model employed is a conceptually simple one on an  $f$ -plane, consisting of a cylindrical basin of uniform depth which is connected to an 'open ocean' through two shallow passages. The fluid motion is driven by applying a uniform cooling at a portion ( $1/4$ ) of the basin's vertical sidewall. The sidewall cooling is much easier to control than the more realistic way of cooling from above, and that it can produce a localized sinking of cold (dense) water which is an essential part of the oceanic buoyancy forcing. The resultant convective circulations in the model are observed by means of a dye technique over a period of 'stratification time scale'.

On an  $f$ -plane, unlike on a  $\beta$ -plane, there is no definite rule for introducing cardinal points to the system. One natural and meaningful way of doing so is to regard the cooled portion of the basin as "north" ("south") for the northern (southern) hemisphere basic rotation; other directions are then automatically determined. In what follows, we will follow this rule and

---

\* Research Institute for Applied Mechanics, Kyushu University, Kasuga 816, Japan.

directions thus introduced will be distinguished by attaching a quotation mark " " as "west" or "western". In most experiments one passage is made on the "west" side of the inner basin and the other is on the "east" side to model the basic configuration of the Japan Sea. If the "eastern" passage is closed, the model mimics the Mediterranean Sea with the Strait of Gibraltar. Experiments are carried out also for this version with a single passage to see the possible effect of the northern sinking in the Mediterranean Sea on the water exchange processes through the Strait of Gibraltar.

## 2. Description of experiments

A top view of the laboratory model is schematically shown in Fig. 1. The model consists of a plexiglass cylindrical container (40 cm in diameter) placed centrally in another container (60 cm in diameter). The inner basin is connected to the outer one (an 'open ocean') through two shallow passages with a width of 5 cm (about 5 times the internal radius of deformation). A portion (1/4) of the annulus region between the two cylindrical containers is partitioned by two *insulated* vertical plates so that the water temperature in this portion can be varied independently of the remainder. The working fluid then occupies the remaining portion (3/4) of the annulus region and the inner basin to a constant depth (mostly 8 cm). These working basins are further set in a larger water tank (80 cm in diameter) to minimize the effect of the change in room temperature on the working fluid; otherwise, the sidewall of the outer basin is directly exposed to the temperature change, which readily gives rise to unwanted convective motions in the annulus region and then in the inner basin. Initially all the water temperatures in the apparatus were set at a fixed value, say  $T_0$ , and the top of the working basin was covered with a lucite plate to prevent the air from exerting a stress on the free surface of the working fluid (the gap between the top cover and the free surface was less than 1 cm). The whole apparatus was mounted on a turntable and set rotating in the counter-clockwise direction about its vertical axis of symmetry. After the working fluid attained a complete solid-body rotation (this was checked by

releasing dye-lines), the water temperature in the partitioned (1/4) portion of the annulus region was lowered by  $\Delta T_0$  by adding chilled water to the "northern" cooling zone and was kept at the lowered value ( $T_0 - \Delta T_0$ ) throughout the duration of each experimental run, while the water temperature in the outermost tank was kept constant at the initial value  $T_0$ . This allowed us to impose a well-controlled local cooling on the vertical sidewall of the inner basin. Experiments were conducted only when the room temperature was slightly (by less than  $0.5^\circ\text{C}$ ) higher than the basin water temperature; otherwise, the top cover of the working basin would be dimmed with water vapor. Hence the working fluid was subject to heating from above. Repeated checks by dye lines showed that the uniform heating from above alone induced no appreciable motion in the basin.

The convective motion thus induced in the basin was observed by a dye technique. For this purpose, a diluted solution of thymol blue (a pH indicator) was used as the working fluid and several electrodes of 0.005 cm platinum wire were stretched horizontally at desired locations and depths. A standard arrangement of dye wires is sketched in Fig. 1, where the lower dye wire is at 1.5 cm above the bottom plate and others are at the mid-depths of the inner basin and the passages. A movable vertical electrode

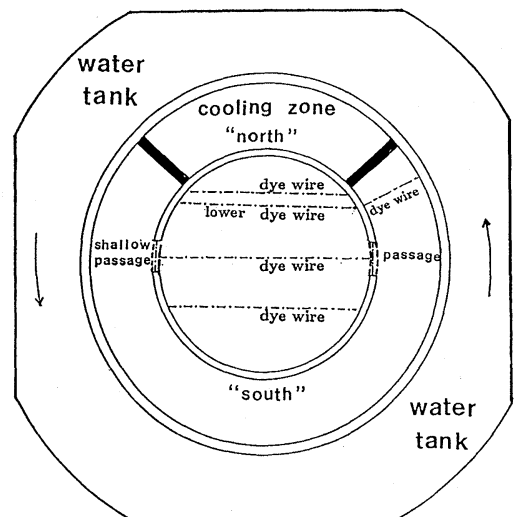


Fig. 1. Top view of the experimental set-up on a turntable.

of 0.05 cm copper wire was also used to survey the vertical profile of the flow. When a d.c. potential ( $\sim 15$ v) was applied across the electrodes, blue dye was swept off each electrode by flow. Resulting dye patterns were photographed by a camera mounted on the turntable. The temperature of the working fluid was measured by a thermister at the foot of the cooled ("northern") sidewall where the coldest water mass was found.

The controllable external parameters are the basic rotation rate  $\Omega$ , the applied temperature difference  $\Delta T_0$  and the height of the working fluid  $H$ . Values of these parameters were

$$\Omega = 0.1 \sim 0.5 \text{ rad/s}, H = 8 \text{ cm}, \\ \Delta T_0 = 0.5 \sim 1.5^\circ\text{C} \text{ (for } T_0 = 15^\circ\text{C typically)}.$$

The depth of the passages was set to be  $H/2$  ( $= 4$  cm). It should be noted here that the effective temperature difference imposed on the working fluid was much smaller than  $\Delta T_0$  due to highly insulating nature of the sidewall material (0.8 cm-thick plexiglass); temperature measurements showed that it was about one third of  $\Delta T_0$ . Then we will use  $\Delta T = \Delta T_0/3$ , rather than  $\Delta T_0$  itself, as a measure of the thermal forcing. In terms of these external parameters, a propagation speed of the density difference, the internal radius of deformation and the buoyancy frequency are given respectively as

$$c = \sqrt{g \cdot \alpha \cdot \Delta T \cdot H}, \quad \lambda = c/2\Omega \\ \text{and } N = \sqrt{g \cdot \alpha \cdot \Delta T/H},$$

where  $g$  is the gravitational acceleration and  $\alpha$  the thermal expansion coefficient (which depends on the fluid temperature). Values of these basic quantities were typically (e.g., for  $\Delta T_0 = 1.0^\circ\text{C}$ ,  $T_0 = 15^\circ\text{C}$ ,  $\Omega = 0.3$  rad/s)

$$c = 0.6 \text{ cm/s}, \quad \lambda = 1 \text{ cm}, \quad N = 0.08 \text{ s}^{-1}.$$

Related non-dimensional quantities are the Ekman number  $E$ , the Burger number  $S$  and the Rayleigh number  $Ra$ , which are respectively defined as

$$E = \nu/2\Omega H^2, \quad S = (N/2\Omega)^2 \cdot (H/L)^2 = (\lambda/L)^2, \\ \text{and } Ra = g\alpha \Delta T H^3/\nu \kappa,$$

where  $L$  is the diameter of the inner working basin and  $\kappa$  the thermal diffusivity. Most

experiments were conducted under the following conditions:

$$E = 10^{-4} \sim 10^{-3}, \quad S = 10^{-4} \sim 10^{-3}, \quad Ra = 10^6 \sim 10^7.$$

Before describing the experimental results, we will refer to the time scales relevant to the thermal motion. The shortest one is the time for the density difference to propagate (as Kelvin waves) over a significant distance of the working basin, which may be given as  $\tau_1 = L/c$ . The phenomenon under consideration is a typical 'filling box' process (TURNER, 1979). As is well known (see, e.g., WORSTER, and LEITCH, 1985; CONDIE, 1989), the most important time scale for general 'filling box' problems is the time to pump all the working fluid through vertical boundary layers along cooled (or heated) sidewalls. This so-called 'stratification time scale' is defined for the present configuration as

$$\tau_2 = L \cdot H / \kappa Ra^{1/4}.$$

The longest time scale is the thermal diffusion time  $\tau_3 = H^2/\kappa$ . The momentum diffusion time  $\tau'_3 = H^2/\nu$  is much smaller than  $\tau_3$  since  $\nu \gg \kappa$  for the working fluid. Another diffusive time worth noting is a damping time of the Kelvin wave,  $\tau_4 = \lambda^2/\nu$ . Values of these time scales were typically  $\tau_1 \sim 1$  min,  $\tau_4 \sim 2$  min,  $\tau_2 \sim 1$  hour,  $\tau'_3 \sim 2$  hours and  $\tau_3 \sim 12$  hours. The duration of each experimental run was about 3 hours, i.e.  $3\tau_2$ .

### 3. Experimental results

When the differential cooling is applied, working fluid adjacent to the cooled ("northern") portion of the basin's sidewall sinks to the bottom through a thin vertical boundary layer and flows away from the source region in a density current. Under the rotational constraint (the basic rotation is anti-clockwise), the density current is deflected to the right (facing downstream) to form a narrow boundary current flowing anti-clockwise along the periphery of the bottom layer. Because of damping effect the density-driven deep current is stronger on the "western" side than on the downstream "eastern" side, exhibiting an "east-west" asymmetry. The object of major interest here is the compensatory circulation in the upper-layer and the associated in- and outflow phenomena between the

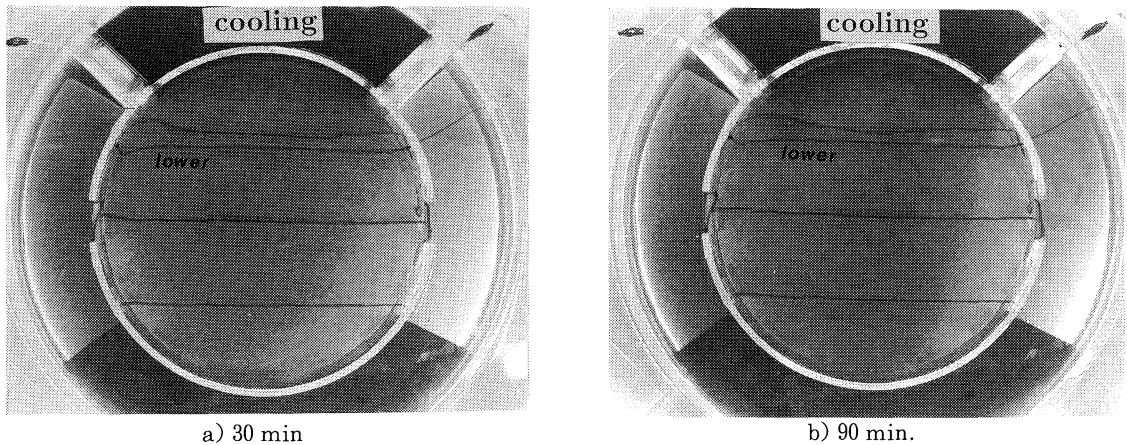


Fig. 2. A basin-wide circulation and an in- and outflow through the two passages induced by the sidewall cooling:  $\Omega = 0.140$  rad/s,  $\alpha \Delta T = 0.30 \times 10^{-4}$ . The lower dye wire is at 1.5 cm above the bottom and others are at the mid-depths of the basin and the passages. Interval between dye pulses is 1 min.

inner basin and the surrounding basin.

Figures 2a), b) are typical examples of the convective circulation as visualized by horizontal dye lines at two different times after the onset of the differential cooling. The basin-wide circulation in the inner basin is essentially similar to the one in the absence of the passages which has been described in some detail in a previous paper (TAKEMATSU, 1991). It consists of an anti-cyclonic major gyre with a "westward" intensified boundary current and a "western" deep counter-current from the sinking region. [The deep boundary current is not visible on the "eastern" side due to a relatively large damping ( $\tau_d / \tau_i \sim O(1)$ ).] Note in particular that the compensating surface boundary current is much stronger and wider than the underlying boundary current of "northern" origin. The net horizontal transport in the "western" boundary region is apparently "northward". It is also worth nothing that the surface "western" boundary current naturally separates from the side boundary in the "northern" region where sinking is produced. A new and important feature demonstrated in Fig. 2 is the marked inflow through the "western" shallow passage. Survey by a vertical (movable) electrode showed that the inflow at the passage was almost barotropic although it had a slight vertical shear decreasing downwards. [If the passage were fully open to the bottom, the cold deep water of "nor-

thern" origin would spill out of the inner basin through the passage and this would alter the entire flow pattern.] It is remarkable that the buoyancy-driven inflow is not uniform across the "western" passage; the inflow is much stronger in the "northern" part of the passage than in the "southern" part, having the maximum speed near the "northern" end of the passage. The maximum speed of the inflow is comparable to that of the surface "western" boundary current towards the sinking region. The net inflow through the "western" passage is balanced by the same amount of outflow through the "eastern" passage. This exchange of fluid in the inner basin is accompanied with a recirculating flow from the "eastern" to "western" passage in the annulus region (this was confirmed in preliminary experiments). It should be noted that the cooling of the inner basin had no *direct* influence on the fluid in the annulus region: Indeed the "northern" ends of the annulus near the cooling zone were always motionless as may be seen from the dye line across the annulus.

Figure 3 shows a horizontal circulation pattern for a different rotation rate  $\Omega = 0.419$  rad/s. The general features are similar to those in Fig. 2 for  $\Omega = 0.140$  rad/s except that the widths of the "western" boundary current, deep counter-current and the inflow are all smaller than the corresponding widths in Fig. 2. These

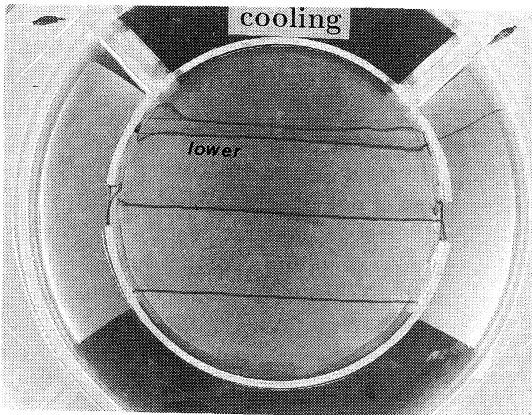


Fig. 3. A basin-wide circulation and an in- and outflow at 150 min for a different rotation rate:  $\Omega = 0.419$  rad/s,  $\alpha \Delta T = 0.30 \times 10^{-4}$ . Dye interval, 1.5 min.

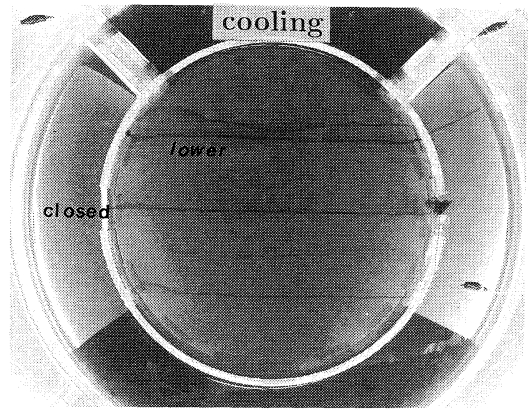


Fig. 5. A photograph illustrating the absence of an in- and outflow through the single "eastern" opening. The experimental conditions are the same as those in Fig. 4.

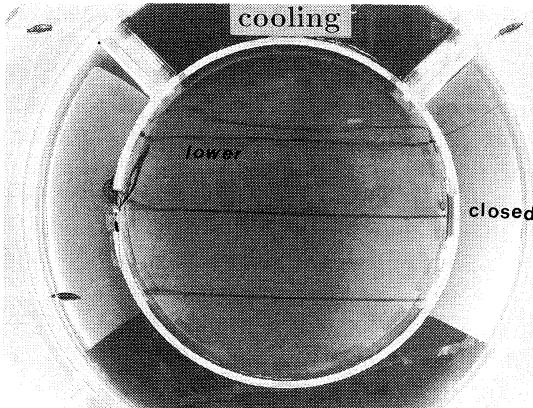


Fig. 4. A surface inflow and a compensatory outflow in the lower layer through the single "western" opening:  $\Omega = 0.140$  rad/s,  $\alpha \Delta T = 0.67 \times 10^{-4}$ .

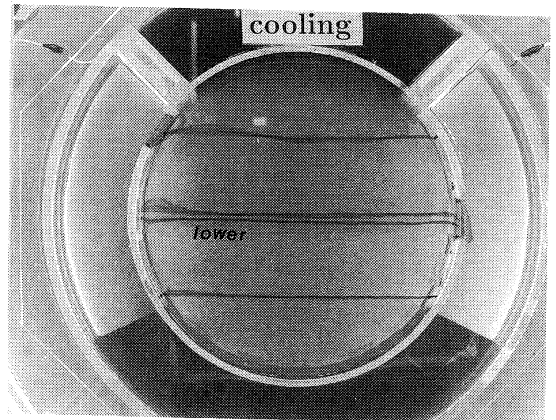


Fig. 6. An intense inflow through a "western" passage opening located very near to the sinking region. The experimental conditions are almost the same as those in Fig. 2b). Interval between dye pulses is 0.75 min (45 sec).

current widths seem to vary in proportion to the radius of deformation  $\lambda$ : Indeed, values of  $\lambda$  in Figs. 2 and 3 are 1.7 cm and 0.7 cm respectively, and the corresponding widths of the inflow are 5 cm and 2 cm (about  $3\lambda$ ).

Experiments for the case of a single passage are also suggestive. Figure 4 illustrates a feature of the flow through the "western" passage when the "eastern" one is closed (a configuration relevant to the Mediterranean Sea). The dye pattern released from a vertical electrode at the center of the "western" passage shows that an inflow occurs only in the upper layer of the passage and this surface inflow is replaced by a

lower-layer outflow from the inner basin. For comparison, a typical example of flow patterns in the basin with a single "eastern" passage is shown in Fig. 5. The dye released at the passage is only lingering around the source region, indicating that there is no appreciable in- and outflow through the single "eastern" passage. This feature contrasts with the prominent in- and outflow through the single "western" passage. These experiments with a single passage indicate that the "eastern" passage plays only a passive role in the buoyancy-driven in- and outflow

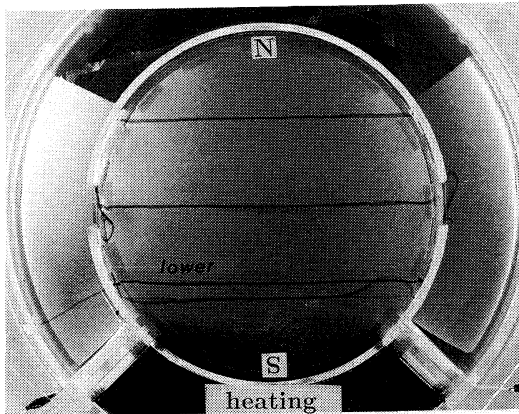


Fig. 7. An in- and outflow through the two openings induced by heating a "southern" portion of the basin's sidewall:  $\Omega = 0.419$  rad/s,  $\alpha \Delta T = 0.63 \times 10^{-4}$  (heating). Dye interval, 1.5 min.

processes. This is presumably because the effects of "northern" cooling which propagate anti-clockwise effectively damp out before reaching the "eastern" side of the basin. The "northern" sinking, affected by Coriolis forces and damping effects, appears to act as a non-isotropic sink (biased towards "west") for the upper layer of the basin. It may be this "westward" intensified sink-effect that drives the surface inflow in Fig. 4 as well as the nearly barotropic inflow in Figs. 2 and 3. In this respect the inflow feature illustrated in Fig. 6 is noteworthy, where the passage on the "west" side has been approached to the sinking region. It can be seen that the inflow through the "north-west" passage is stronger than that through the due "west" passage in Fig. 2b).

In an additional experiment the water temperature of the cooling zone was raised, rather than lowered. A resulting horizontal circulation pattern is shown in Fig. 7, where the heating zone is regarded as "south". The localized rising of warm fluid along the heated sidewall causes a basin-wide cyclonic gyre in the inner basin and an in- and outflow through its two passages. It is remarkable that the inflow occurs again through the "western" passage as in the case of "northern" cooling. In another additional experiment, the working fluid was subjected to a uniform cooling from above (by lowering the room temperature) as the Japan Sea would be

during the last Ice Age, and it was confirmed that uniform cooling from above induces no appreciable mean currents either in the inner basin or around the passages.

Evolution characteristics of the buoyancy-driven motion are also worth noting. Dye observations carried out at specially short intervals (5~10 min) showed that the basin-wide circulation including the in- and outflow develops very rapidly during about 20 min after the onset of the thermal forcing. An apparent inflow was seen even at the first 5 min ( $\sim 5 \tau_1$ ); the convective motion at this earliest stage was still weak, but it possessed all essential features of the fully developed one. The in- and outflow as well as the circulation in the inner basin then gradually evolve over a period of 90 min ( $\sim \tau_2$ ). Evolution of the convective motion at this second stage is illustrated in Figs. 2a) and 2b). Note in particular that the flow field at 30 min (Fig. 2 a)) is already very similar to the fully developed one at 90 min (Fig. 2b)). During the subsequent 90 min no appreciable change was observed in the flow features. After a period of the longest time-scale  $\tau_3$ , however, the density field as well as the velocity field in the basin are supposed to approach gradually a final steady state that depends on the room temperature and the thermal boundary conditions of the basin (insulated or isothermal).

#### 4. Summary and concluding remarks

The laboratory experiments on an f-plane with the northern-hemisphere rotation have revealed some new aspects of a convective motion in a rotating basin which is connected to an open ocean through shallow passages. An important finding is that a localized sinking in a "northern" area of the basin produces not only a basin-wide circulation with a "western" boundary current but also an inflow from an open ocean if there is a shallow passage on the "west" side of the basin. The buoyancy-driven inflow is characterized by a marked "north-south" asymmetry across the passage; it is concentrated in the "northern" portion of the passage. The entire convective motion manifests itself very soon ( $\sim 5 \tau_1$ ) after the onset of the differential cooling and gradually evolves on longer time scales ( $\tau_2$  and  $\tau_3$ ). The experiments have been conducted

only within the laminar-flow regime and rather restricted ranges of parameters, but the major flow features are expected to be similar for wider ranges of flow conditions. More detailed study of the quantitative aspects of the buoyancy-driven in- and outflow is now under way and will be published elsewhere.

The buoyancy-driven inflow process demonstrated herein may be oceanically relevant. We have in mind the winter-time sinking of dense water in the northern part of the Japan Sea or of the Mediterranean Sea. The present study suggests that such a localized sinking may induce a nearly barotropic inflow through the Korea/Tsushima Strait and a surface inflow through the Gibraltar Strait. Since sinking phenomena in reality are intermittent, the resultant inflow and the compensatory outflow would also be intermittent. In this respect it should be recalled that the basin-wide circulation as well as the inflow appear very soon (within a period of  $5 \tau_1$  or so) after the onset of sinking. In real marginal seas  $\tau_1$  is of the order of 10 days. Then it seems likely that the in- and outflow processes can feel the seasonal change in the rate of sinking.

### References

- CONDIE, S.A. (1989): A Laboratory Model of a Convectively Driven Ocean. *Dyn. Atmos. Ocean*, **13**, 77-93.
- FANG, G., B. ZHAO and Y. ZHU (1991): Water Volume Transport through the Taiwan Strait and the Continental Shelf of the East China Sea Measured with Current Meters. *In Oceanography of Asian Marginal Seas (Proc. 5th JECSS workshop)*, ed. K. TAKANO, Elsevier Oceanogr. Ser., **54**, 345-358.
- MINATO, S. and R. KIMURA (1980): Volume Transport of the Western Boundary Current Penetrating into a Marginal Sea. *J. Oceanog. Soc. Japan*, **36**, 185-195.
- SEKINE, Y. (1988): On the Seasonal Variation in In- and Outflow Volume Transport of the Japan Sea. *Prog. Oceanog.*, **21**, 269-279.
- TAKEMATSU, M. (1991): Western Intensification of Buoyancy-Driven Ocean Currents. *Rep. Res. Inst. Appl. Mech., Kyushu Univ.*, **38**, No. 108, 37-47.
- TOBA, Y., K. TOMIZAWA, Y. KURASAWA and K. HANAWA (1982): Seasonal and Year-to-Year Variability of the Tsushima-Tsugaru Warm Current System with its Possible Cause. *La mer*, **20**, 40-51.
- TURNER, J.S. (1979): *Buoyancy Effects in Fluids*. Cambridge Univ. Press.
- WORSTER, M.G. and A.L. Leitch (1985): Laminar Free Convection in Confined Regions. *J. Fluid Mech.*, **156**, 301-319.